Available online at www.sciencedirect.com
SCIENCE DIRECT®
Acta Materialia 52 (2004) 4305–4315
Acta MATERIALIA
www.actamat-journals.com

Suppression of intermediate phase nucleation in binary couples with metastable solubility

F. Hodaj [a,*], A.M. Gusak [b]

[a] Laboratoire de Thermodynamique et Physico-Chimie Métallurgiques, CNRS URA 29, Institut National Polytechnique de Grenoble, BP 75, 38402 Saint Martin dHeres, France
[b] Department of Theoretical Physics, Cherkasy National University, Shevchenko Street 81, Cherkasy 18000 Ukraine

Received 11 October 2003; received in revised form 21 May 2004; accepted 27 May 2004

Abstract

This paper investigates the influence of sharp concentration gradients and/or chemical potentials on the nucleation of intermediate phases during solid state reactions between elements with limited solubility. These factors would not appear to have any significant influence on first intermediate phase nucleation. On the other hand, for the second and subsequent phases, thermodynamic suppression (in addition to the kinetic factor) of nucleation can be quite considerable and may well be the reason for sequential phase formation in thin films. Thermodynamic suppression criteria for intermediate phase nucleation are proposed.

Keywords: Nucleation; Thermodynamics; Diffusion; Phase formation; Thin films

1. Introduction

It has been well known for several decades that reactive diffusion in thin films usually demonstrates "one-by-one" (sequential) phase formation [1,2]. Despite the existence of several stable intermediate phases on the phase equilibrium diagram, only one growing phase layer between end members of the couple is usually observed. The next phase appears, or at least becomes visible, after one of the terminal materials has been consumed, so that the first phase has no more material for growth, becoming itself a material for second phase formation, and so on. Such sequential growth has at least three possible explanations:

(a) "*Just slow growth*". The first phase to grow usually has the maximum diffusivity and, hence, grows fast (according to F.d'Heurle [2], "fast is the first" or "first is fast"). Other phases, with lower diffusivities, grow even slower than they could do alone, without a fast growing neighbor. Growth rate of phase layers with very narrow homogeneity regions $C_{i\mathrm{R}} - C_{i\mathrm{L}} = \Delta C_i \ll 1$ is determined by the combination of so-called Wagner diffusivities $D_i\Delta C_i = \int_{C_{i\mathrm{L}}}^{C_{i\mathrm{R}}} \tilde{D}(C)\,\mathrm{d}C$, which are proportional to the product of combination of self-diffusivities inside each phase and the thermodynamic driving force of phase formation (C-atomic fraction of B-component, $\tilde{D}(C)$ – interdiffusion coefficient [3]). For example, in the case of two simultaneously growing phases 1 and 2, with significantly different integrated Wagner diffusivities $D_1\Delta C_1 \gg D_2\Delta C_2$ (under condition of negligible solubility of A in B and B in A) their thickness ΔX_i obeys the following parabolic laws (omitting factors of about unity): $\Delta X_1 \approx \sqrt{2D_1\Delta C_1}t^{1/2}$, $\Delta X_2 \approx 2D_2\Delta C_2/(\sqrt{2D_1\Delta C_1})t^{1/2}$, so that $\Delta X_2/\Delta X_1 \approx D_2\Delta C_2/D_1\Delta C_1$. (Note that in the absence of a fast phase 1, the second phase would grow much faster: $\Delta X_2^{\mathrm{single}} \approx (\sqrt{2D_2\Delta C_2})t^{1/2}$). Thus, according to this first explanation, other phases exist and grow, but too slowly, and their layers are so thin, that it is just difficult to detect them.

* Corresponding author. Tel.: + 33-4-76-82-65-15; fax: +33-4-76-82-67-67.
E-mail address: fhodaj@ltpcm.inpg.fr (F. Hodaj).

1359-6454/$30.00 © 2004 Acta Materialia Inc. Published by Elsevier Ltd. All rights reserved.
doi:10.1016/j.actamat.2004.05.047

(b) *Diffusive suppression of critical nuclei* [4–6]. Any phase can start growing only from nuclei of a certain critical size l_{cr}. Yet, since these nuclei (created as a result of inevitable heterophase fluctuations) are from the very beginning situated in the sharply inhomogeneous system and, hence, take part in diffusive interactions, they can shrink to undercritical (unstable with respect to dissolution) size due to diffusive suppression of the neighboring, fast growing phase. Such diffusive suppression of second phase critical nuclei takes place if the thickness of first phase is less than $\Delta X_1^* = [(1-C_2)/(1-C_1)](D_1\Delta C_1/D_2\Delta C_2)l_{cr}^{(2)}$. Thus, before the first phase layer reaches this critical thickness, this "vampire" phase suppresses all nucleation attempts of phase 2, so that the latter is present only "virtually" and, therefore, it is not being detected.

(c) *Interfacial barriers + competition* [7]. Interfacial barriers are believed to cause the initial linear phase growth. In the case of single-phase formation the interfacial barriers simply slow down the rate of formation, making it linear instead of parabolic. For two phases, the barriers can make the growth rate of a certain phase formally negative even for zero thickness, which means that this phase will be totally absent. Both models [4,7] (published the same year) predict the suppression/growth criterion and a certain critical thickness of the first growing phase under which growth of other phases is kinetically suppressed. Model [7] is very attractive and well known, but the constants of interfacial kinetics are, to our knowledge, adjusting parameters.

In 1990 another approach to the problem of phase competition was simultaneously initiated in [8,9] – taking into account thermodynamic constraints on nucleation, imposed by the sharp concentration gradient ∇C in a diffusion zone. If, prior to intermediate phase formation, a narrow layer of metastable solid solution or amorphous alloy had been formed at the base of the initial interface, the sharp concentration gradient inside this layer would lead to a decrease in the total bulk driving force of nucleation, and a corresponding increase in nucleation barrier:

$$\Delta G(r) = \Delta G^{\text{classic}} + \gamma(\nabla C)^2 \cdot r^5, \tag{1}$$

where $\Delta G(r)$ is the change in Gibbs free energy due to formation of a cubic nucleus of size $2r$ [9] or spherical nucleus of radius r [8] and $\gamma > 0$. Moreover, if the concentration gradient exceeds a certain critical value ∇C_{crit} (and the width of the metastable layer is less than $1/\nabla C_{\text{crit}}$, typically not more than 10 nm), the nucleation barrier tends towards infinity, meaning "thermodynamic" suppression (instead of, or more precisely, prior to kinetic suppression). This approach (as well as approaches [4,7]) had been applied to the description of solid state amorphizing reactions [9–11], explaining why stable intermetallics appear in the diffusion zone only after the amorphous layer exceeds a certain critical thickness.

In spite of similar results, models [8] and [9] of nucleation in the sharp concentration gradient treated quite different possible mechanisms (nucleation modes). In [8] (see also [12]) a *polymorphic (diffusionless) mode* has been suggested according to the following picture: Initial diffusion leads to the formation and growth of a metastable parent solution with sharp concentration profile. When this profile becomes smooth enough to provide sufficient space for compositions favorable for a new intermediate phase, this very phase nucleates just by reconstruction of the atomic order, without immediately changing the concentration profile (at "frozen" diffusion) – polymorphic transformation. In [9,10] the *transversal nucleation mode* was suggested bearing in mind the following picture: Each thin slice of the newly formed nucleus, perpendicular to the direction of concentration gradient, is considered to be the result of decomposition of the corresponding infinite thin slice of parent solution, leading, of course, to redistribution of atoms among new and old phases. In this transversal mode, the redistribution proceeds within each slice, independently of others.

In [13] another mechanism has been suggested (and analyzed in more detail in [6,14]) – *total mixing (longitudinal) nucleation mode*, in which the redistribution of atoms takes place during nucleation, but only inside the newly forming nucleus. Contrary to the two previous modes, in this case the concentration gradient assists nucleation – in expression (1) coefficient γ is negative.

The "natural" thing is to expect that nature will use the mechanism with the lowest nucleation barrier – the total mixing mode. But nucleation is governed not only by thermodynamics but also by kinetics. It has been shown in [6,13] that the relative contribution of each mechanism depends on the ratio of atomic mobilities in the parent and nucleating phases. If atomic mobility in the new phase is much lower than in the parent phase, then the total mixing mode is not going to happen. If the opposite is true (high mobility inside new phase), then nucleation will proceed very quickly by total mixing (again, "fast is first").

All the above-mentioned models treated the case where the system, prior to nucleation, can form a metastable parent phase with a broad concentration range, overlapping the equilibrium concentration range of a new stable phase (Fig. 1(a)). Yet, in most cases the solid state reactions produced in couples with small mutual solubilities even in the metastable state (Fig. 1(b)). In case of phase 1 nucleation between α and β, these phases, in the absence of phase 1, have metastable solubilities C_α^m and $1 - C_\beta^m$. Prior to nucleation the interdiffusion should lead to a step-like concentration profile which has a concentration gap (C_α^m, C_β^m) and, therefore, does not overlap the phase 1 concentration

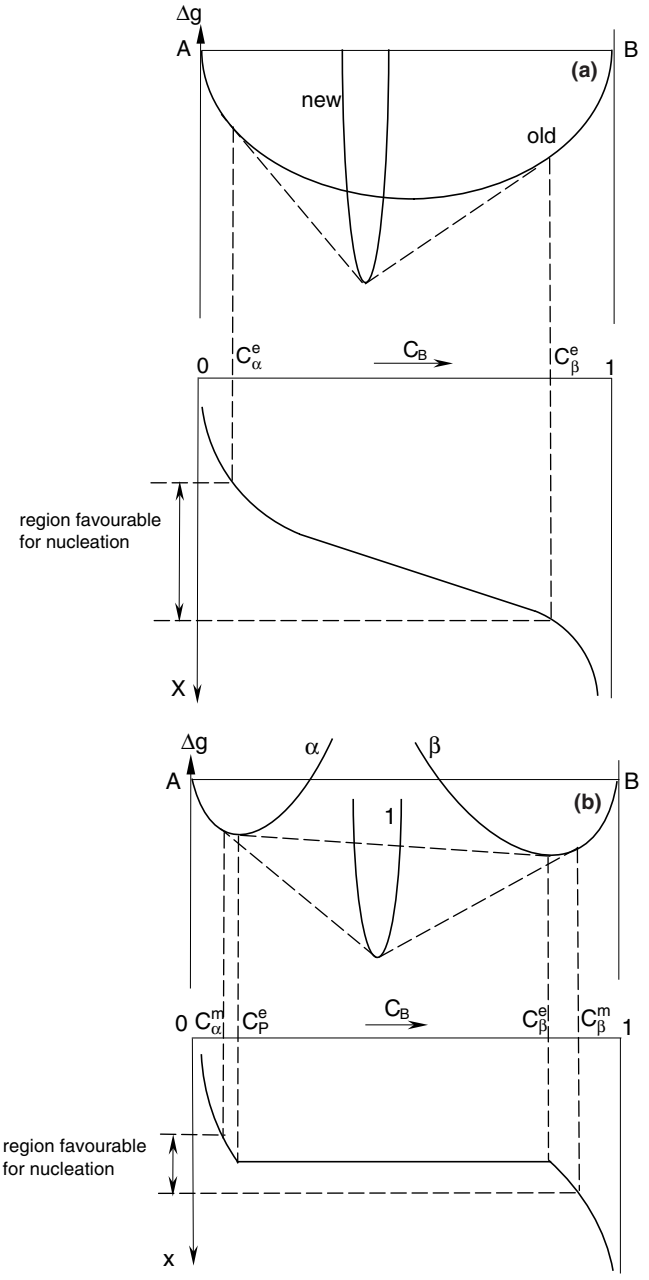

Fig. 1. Schematic "Gibbs free energy versus composition" and corresponding "composition versus diffusion coordinate" dependencies for two cases: (a) intermediate phase homogeneity range is inside the metastable solution range and (b) intermediate phase homogeneity region is outside the metastable solubility limits of both parent phases.

range. In this case the polymorphic mode is, of course, impossible.

The transversal mode, on the contrary, is quite possible and should take place as a simultaneous decomposition of metastable non-homogeneous solutions within concentration intervals (C^e_α, C^m_α) and (C^m_β, C^e_β) on both sides of the interface. Some aspects of this problem, concerning the nucleus shape, have been treated in [15,16]. However, no new conclusions (compared with [9,10]) nor estimates, concerning the suppression of nucleation, have been proposed. Nucleus shape, while being an important nucleation factor in the concentration gradient [6,14,17,18], is not decisive. Therefore, in the present analysis, the shape problem is ignored for the moment, leaving the focus on the "gradient effect" on nucleation barrier.

Thermodynamic considerations for prediction of the phase sequence have been used as well by Lee et al. [19]. Authors took into account the change of driving force due to formation of metastable solution. Yet, they did not take into account the influence of concentration and chemical potential gradients on the driving force.

The main idea of the present paper is that the effect of concentration gradient (or more exactly, chemical potential gradients) should be significant for nucleation in systems with limited metastable solubility, especially when at least one intermediate phase is already growing. It is quite possible that the "gradient approach" in this case can give a key to understanding a sequential phase growth.

Section 2 analyzes the general case of phase "*i*" nucleation at the interface between non-homogenous (with gradients of concentration and of chemical potentials) phase layers L and R. In Sections 3–5, this general formalism is applied respectively to nucleation at the interface between (a) two dilute solutions α and β, (b) two intermediate phases 1 and 3 already growing, and (c) a growing phase 1 and a dilute solution β. Section 6 discusses some applications of these results to the SSR in thin films and multilayers.

2. Nucleation of line compound at the interphase interface during interdiffusion

In this analysis, phases L and R are assumed to have already developed some concentration profiles $C_L(X), C_R(X)$ with concentration gap (C_{LR}, C_{RL}) and metastable regions (C_{Li}, C_{LR}) and (C_{RL}, C_{Ri}), conducive to the nucleation of line compound "*i*" (Fig. 2). The change in Gibbs free energy due to nucleation (by transversal mode) of a parallelepiped of new phase $2h \times 2h \times 2r$ can be determined, where $2h$, r are respectively the size in the lateral (Y and Z axes) and the gradient or longitudinal (X-axis) directions. The longitudinal size $2r$ consists of parts overlapping the phases L and R and originating from these phases: $2r = r_L + r_R$. Then:

$$\Delta G = 4h^2(\sigma_{iL} + \sigma_{iR} - \sigma_{LR}) + 4 \cdot 2h(r_L\sigma_{iL} + r_R\sigma_{iR}) + \frac{1}{\Omega}\int_{y-r_L}^{y} \Delta g(C_L(X) \to C_i) \cdot 4h^2 dX + \frac{1}{\Omega}\int_{y}^{y+r_R} \Delta g(C_R(X) \to C_i) \cdot 4h^2 dX. \quad (2)$$

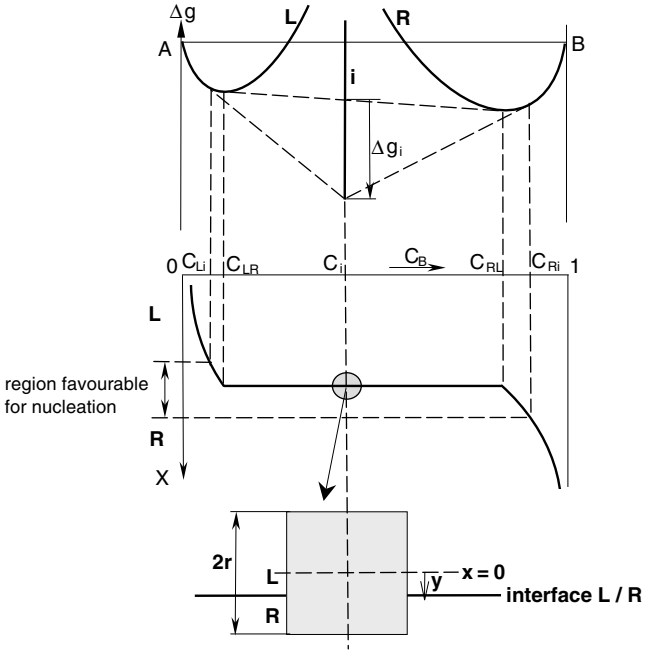

Fig. 2. Schematic representation of intermediate phase nucleation at the L/R interface with L and R being the parent phases. Δg_i is a driving force per mole of atoms for the $L + R \rightarrow i$ reaction. Distribution of nucleus volume among phases is determined by additional optimization procedure (Eqs. (8) and (9)).

Here, Ω is an atomic volume of phase "i", $\sigma_{iL}, \sigma_{iR}, \sigma_{LR}$ are corresponding surface tensions, y is the position of L/R interface with respect to the x-axis ($x = 0$ at the center of the embryo). Driving forces per atom of nucleus for precipitation of $L^{metast} \rightarrow i$ and $R^{metast} \rightarrow i$ are expressed by the "parallel tangents rule" (not to be confused with "common tangent rule") [10]; for $L^{metast} \rightarrow i$:

$$-\Delta g(C_L(X) \rightarrow C_i) = g_L(C_L(X)) - g_i - (C_L(X) - C_i)\frac{\partial g_L}{\partial C}\Big|_{C=C_L(X)}, \quad (3)$$

(For $R^{metast} \rightarrow i$ by analogy).

In addition, expansions into Taylor series are used both for concentrations and for Gibbs free energies per atom:

$$C_L(X) \approx C_L(y) + (X - y)\cdot\nabla C_L\Big|_{X=y-0}, \quad \text{for } X < y,$$

$$C_R(X) \approx C_R(y) + (X - y)\cdot\nabla C_R\Big|_{X=y+0}, \quad \text{for } X > y, \quad (4)$$

$$g_L(C_L) \approx g_L(C_{LR}) + (C_L - C_{LR})g'_L + \frac{(C_L - C_{LR})^2}{2}g''_L,$$

$$g_R(C_R) \approx g_R(C_{RL}) + (C_R - C_{RL})g'_R + \frac{(C_R - C_{RL})^2}{2}g''_R. \quad (5)$$

Here the first and second derivatives of the concentration are taken at the metaequilibrium compositions C_{LR}, C_{RL} (see Fig. 2). Substitution of Eqs. (4) and (5) into Eq. (3), and then of Eq. (3) into Eq. (2) gives, after simple but long algebra:

$$\begin{aligned}\Delta G = {} & \left[4h^2(\sigma_{iL} + \sigma_{iR} - \sigma_{LR}) + 4\cdot 2h(r_L\sigma_{iL} + r_R\sigma_{iR})\right] \\ & + \Delta g_i\cdot\frac{4h^2}{\Omega}\cdot(r_L + r_R) + \frac{2h^2}{\Omega}\cdot\left[(C_i - C_{LR})g''_L\nabla C_L r_L^2\right. \\ & \left. + (C_{RL} - C_i)g''_R\nabla C_R r_R^2\right] \\ & + \frac{2h^2}{3\Omega}\cdot\left[g''_L(\nabla C_L)^2 r_L^3 + g''_R(\nabla C_R)^2 r_R^3\right]. \end{aligned} \quad (6)$$

Here $(-\Delta g_i)$ is a driving force of the reaction $L + R \rightarrow i$ per atom of i. The first two terms in Eq. (6) represent the classic model of heterogeneous nucleation $\Delta G^{classic}$ (without, however, taking into account Young's equilibrium conditions at three-phase junctions – otherwise a non-symmetrical cap would be obtained with much less transparent mathematics for the gradient effect). The gradient effect is represented both by linear ∇C terms and by quadratic $(\nabla C)^2$ terms providing respectively fourth and fifth power size dependence. In the case of total metastable solubility, the optimization of nucleation place led to the elimination of the linear terms in concentration gradient [17,20]. In the case of limited solubility, these terms remain and, moreover, may play a decisive role. Indeed, $r_L\nabla C_L$ is evidently less than the metastable composition range $\Delta C_L = C_{LR} - C_{Li}$ of L-phase and $r_R\nabla C_R < \Delta C_R = C_{Ri} - C_{RL}$. If the parent material is considered to be only the phases with small mutual solubility (and is assumed here!), then the $(\nabla C)^2 r^3$ terms can be neglected in comparison with the $(\nabla C)^1 r^2$ terms, since $\nabla C\cdot r \ll 1$. In this case:

$$\begin{aligned}\Delta G = {} & \Delta G^{classic} + \frac{2h^2}{\Omega}\cdot\left[(C_i - C_{LR})g''_L\nabla C_L r_L^2\right. \\ & \left. + (C_{RL} - C_i)g''_R\nabla C_R r_R^2\right]. \end{aligned} \quad (7)$$

Eq. (7) is a basic equation for further analysis.

Minimization of ΔG with respect to r_L or r_R (with fixed sum $2r$), in the particular case of equal surface tensions σ for all interfaces, gives:

$$r_L = 2r\frac{\Lambda}{1+\Lambda}, \quad r_R = 2r\frac{1}{1+\Lambda}, \quad (8)$$

with

$$\Lambda = \frac{(C_{RL} - C_i)g''_R\nabla C_R}{(C_i - C_{LR})g''_L\nabla C_L}. \quad (9)$$

Substituting Eqs. (8) and (9) into Eq. (7), the following expression is obtained for the change in Gibbs free energy due to nucleation:

$$\Delta G = \Delta G^{classic} + \frac{8h^2r^2}{\Omega}\cdot\frac{A_L A_R}{A_L + A_R}, \quad (10)$$

with

$$A_{\mathrm{L}} = (C_i - C_{\mathrm{LR}})g''_{\mathrm{L}}\nabla C_{\mathrm{L}}, \quad A_{\mathrm{R}} = (C_{\mathrm{RL}} - C_i)g''_{\mathrm{R}}\nabla C_{\mathrm{R}}. \tag{11}$$

The values of products $g''\nabla C$ will be most important for estimations. These products will be assessed later in Sections 3–5 but, for the time being, they will be assumed to be known. From Eqs. (8) and (9) it is evident that the nucleus will prefer to overlap more with the smaller gradient term $g''\nabla C$. Also, from Eq. (10) it may be concluded that the gradient contribution to the change in Gibbs free energy is controlled by the lesser of two terms A_{L}, A_{R} determined by $g''\nabla C$ (differences in composition are of the order of unity).

Note that, for the simplest case of cubic shape, $h = r$, and for limited solubility within the parent phase (instead of Eq. (1) for full solubility within parent phases), the expression for $\Delta G(r)$ is:

$$\Delta G(r) = \Delta G^{\mathrm{classic}} + qr^4 = \alpha r^2 + \beta r^3 + qr^4, \tag{12}$$

with

$$\alpha = 20\sigma, \quad \beta = \frac{8\Delta g_i}{\Omega}, \quad q = \frac{8}{\Omega}\frac{A_{\mathrm{L}}A_{\mathrm{R}}}{A_{\mathrm{L}} + A_{\mathrm{R}}}. \tag{13}$$

Depending on the value of q, the $\Delta G(r)$ dependence can be monotonically increasing (large q – nucleation forbidden), or with a metastable minimum (intermediate values of q), or with a stable minimum (small q, nucleation possible) – Fig. 3. Cross-over to possible nucleation (second minimum at zero level) means:

$$\frac{\partial \Delta G}{\partial r}|_{r^*} = 0, \quad \Delta G(r^*) = 0. \tag{14}$$

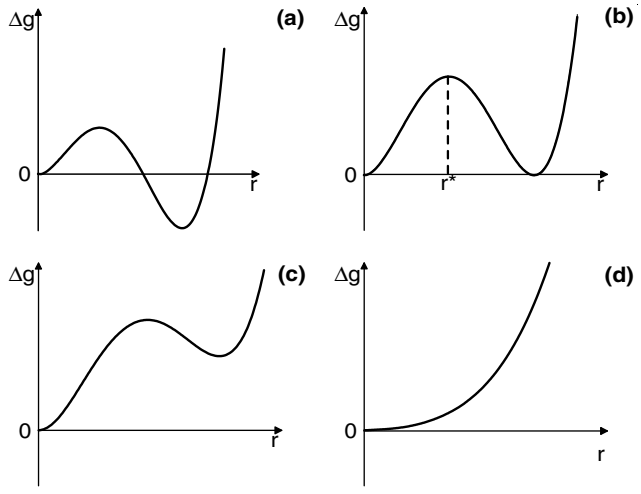

Fig. 3. Schematic "Gibbs free energy change versus nucleus size" dependencies for different values of "gradient term" q (see Eq. (13)): (d) nucleation forbidden ($q > q^{\mathrm{crit}}$), (c) metastable nuclei possible ($q > q^{\mathrm{crit}}$), (b) cross-over to possible nucleation ($q = q^{\mathrm{crit}}$), (a) nucleation possible ($q < q^{\mathrm{crit}}$) (if not suppressed kinetically).

This gives:

$$r^* = \frac{2\alpha}{\beta} = 5\frac{\sigma\Omega}{\Delta g_i}, \quad q^{\mathrm{crit}} = \frac{\beta^2}{4\alpha} = \frac{4(\Delta g_i)^2}{5\sigma\Omega^2}, \tag{15}$$

or

$$\left[\frac{A_{\mathrm{L}}A_{\mathrm{R}}}{A_{\mathrm{L}} + A_{\mathrm{R}}}\right]^{\mathrm{crit}} = \frac{(\Delta g_i)^2}{10\sigma\Omega}. \tag{16}$$

The intermediate phase suppression criterion is then:

$$\frac{A_{\mathrm{L}}A_{\mathrm{R}}}{A_{\mathrm{L}} + A_{\mathrm{R}}} > \frac{(\Delta g_i)^2}{10\sigma\Omega}. \tag{17}$$

Remember that $(-\Delta g_i)$ is a driving force of reaction $\mathrm{L} + \mathrm{R} \rightarrow i$ per atom of i.

The formal approach developed above will be applied in the following sections to different types of adjacent phases L and R.

3. Nucleation between dilute solutions

Let α and β be dilute solutions of B in A and of A in B respectively with solubilities (prior to phase "i" formation) $C^{\mathrm{m}}_{\alpha} \ll 1$ and $(1 - C^{\mathrm{m}}_{\beta}) \ll 1$. Then $g''_{\alpha} \approx \frac{k_{\mathrm{B}}T}{C^{\mathrm{m}}_{\alpha}}$ and $g''_{\beta} \approx \frac{k_{\mathrm{B}}T}{1-C^{\mathrm{m}}_{\beta}}$ can be estimated. The concentration gradients $\nabla C_{\alpha}, \nabla C_{\beta}$ at the α/β moving boundary ($\alpha = \mathrm{L}$ and $\beta = \mathrm{R}$) can be determined from the usual Stephan problem [21]. In general, the solution gives transcendent equations for determining the velocity and parameters of profiles. However, if the difference between $C^{\mathrm{m}}_{\alpha}\sqrt{D_{\alpha}}$ and $(1 - C^{\mathrm{m}}_{\beta})\sqrt{D_{\beta}}$ (D_{α}, D_{β} being the diffusivities in the respective solutions) is not large, then the following approximate expressions can be taken:

$$\nabla C_{\alpha} \approx \frac{C^{\mathrm{m}}_{\alpha}}{\sqrt{\pi D_{\alpha}t}}, \quad \nabla C_{\beta} \approx \frac{1 - C^{\mathrm{m}}_{\beta}}{\sqrt{\pi D_{\beta}t}}, \tag{18}$$

so that

$$g''_{\alpha}\nabla C_{\alpha} \approx \frac{k_{\mathrm{B}}T}{\sqrt{\pi D_{\alpha}t}}, \quad g''_{\beta}\nabla C_{\beta} \approx \frac{k_{\mathrm{B}}T}{\sqrt{\pi D_{\beta}t}}. \tag{19}$$

Therefore:

$$\left(\frac{A_{\alpha}A_{\beta}}{A_{\alpha} + A_{\beta}}\right) \approx \frac{C_i(1 - C_i)k_{\mathrm{B}}T}{\sqrt{\pi D_{\alpha}t}\cdot(C_i\sqrt{D_{\beta}/D_{\alpha}} + 1 - C_i)}.$$

Then, according to Eq. (17), nucleation becomes possible at

$$\frac{C_i(1 - C_i)k_{\mathrm{B}}T}{\sqrt{\pi D_{\alpha}t}\cdot(C_i\sqrt{D_{\beta}/D_{\alpha}} + 1 - C_i)} < \frac{(\Delta g_i)^2}{10\sigma\Omega},$$

or

$$C_i\cdot\sqrt{\pi D_{\beta}t} + (1 - C_i)\cdot\sqrt{\pi D_{\alpha}t} > 5C_i\frac{k_{\mathrm{B}}T}{\Delta g_i}l_i^{\mathrm{cr}}, \tag{20}$$

where $l_i = 2\sigma\Omega/\Delta g_i$ is a standard critical size of nucleus, usually less than 1 nm. The ratio $k_{\mathrm{B}}T/\Delta g_i$ is usually significantly less than unity. This means that nucleation

becomes possible when at least one of two penetration depths reaches nanometric thickness. Thus, in this case nucleation is practically not suppressed.

4. Nucleation between two growing intermediate phase layers

Let L and R be the intermediate phases 1 and 3, growing simultaneously between almost mutually insoluble materials A and B. Here the nucleation of phase 2 at the interface 1/3 is studied (Fig. 4). It is assumed that 1, 2 and 3 are line compounds. In this case, it is more convenient to treat the chemical potential gradients instead of the concentration gradient. Mathematically this gives the following expression:

$$g_1''\nabla C_1 = \frac{\partial}{\partial X}\left(\frac{\partial g_1}{\partial C}\right) \approx \frac{\frac{\partial g_1}{\partial C}\Big|_{13} - \frac{\partial g_1}{\partial C}|_{1\alpha}}{\Delta X_1} = \frac{\frac{g_3-g_1}{C_3-C_1} - \frac{g_1-g_2^{\mathrm{m}}}{C_1-0}}{\Delta X_1}\frac{C_3}{C_1(C_3-C_1)}\frac{(-\Delta g_{10})}{\Delta X_1}, \quad (21)$$

where $(-\Delta g_{10})$ is a driving force of reaction $\mathrm{A}+3\rightarrow 1$ (see Fig. 4). Similarly:

$$g_3''\nabla C_3 = \frac{1-C_1}{(1-C_3)(C_3-C_1)}\frac{(-\Delta g_{30})}{\Delta X_3}, \quad (22)$$

where $(-\Delta g_{30})$ is a driving force of reaction $1+\mathrm{B}\rightarrow 3$. Thus, in this case:

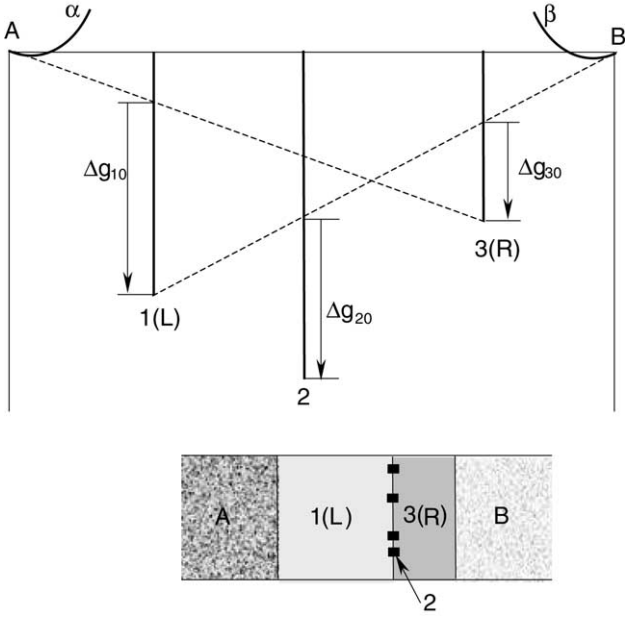

Fig. 4. Schematic representation of phase 2 nucleation between phases 1 and 3, already growing in A/B couple. Δg_{10}, Δg_{30}, Δg_{20} are the driving forces per mole of atoms for the reactions $\mathrm{A}+\mathrm{B}\rightarrow 1$, $\mathrm{A}+\mathrm{B}\rightarrow 3$ and $1+3\rightarrow 2$ respectively.

$$A_{\mathrm{L}} = A_1 = w_1\frac{(-\Delta g_{10})}{\Delta X_1}, \quad A_{\mathrm{R}} = A_3 = w_3\frac{(-\Delta g_{30})}{\Delta X_3}, \quad (23)$$

where

$$w_1 = \frac{(C_2-C_1)C_3}{C_1(C_3-C_1)}, \quad w_3 = \frac{(1-C_1)(C_3-C_2)}{(1-C_3)(C_3-C_1)}. \quad (24)$$

The phase 2 suppression criterion (17) can then be easily reduced to the following form:

$$\frac{\Delta g_{10}}{\Delta g_{30}}\frac{\xi_3}{w_3} + \frac{\Delta g_{30}}{\Delta g_{10}}\frac{\xi_1}{w_1} < 5\frac{\Delta g_{10}\Delta g_{30}}{(\Delta g_{20})^2}, \quad (25)$$

where

$$\xi_1 = \frac{\Delta X_1}{\left(\frac{2\sigma\Omega}{\Delta g_{10}}\right)} = \frac{\Delta X_1}{l_1^{\mathrm{cr}}}, \quad \xi_3 = \frac{\Delta X_3}{\left(\frac{2\sigma\Omega}{\Delta g_{30}}\right)} = \frac{\Delta X_3}{l_3^{\mathrm{cr}}}. \quad (26)$$

Note that w_1 and w_3 are of the order of unity.

If phases 1 and 3 are mutually symmetrical ($\Delta g_{10} = \Delta g_{30}, w_1 = w_3$), then criterion (25) is reduced to:

$$\frac{\Delta X_1}{l_1^{\mathrm{cr}}} + \frac{\Delta X_3}{l_3^{\mathrm{cr}}} < 5\frac{(\Delta g_{10})^2}{(\Delta g_{20})^2}, \quad (27)$$

$(-\Delta g_{20})$ is a driving force of reaction $1(L)+3(R)\rightarrow 2$ (see Fig. 4).

If phase 1 is much wider than phase 3, i.e. $\Delta X_1/\Delta X_3 \gg (\Delta g_{10}/\Delta g_{30})^2$, then it can be shown that the nucleation of phase 2 is preferable at the side of phase $1(r_{\mathrm{R}}\approx 0)$, and criterion (24) is reduced to:

$$\frac{\Delta X_1}{l_1^{\mathrm{cr}}} < 5\frac{(\Delta g_{10})^2}{(\Delta g_{20})^2}. \quad (27')$$

Estimations (27, 27′) are very important. They demonstrate that the critical thickness of the first (and fast) growing phase may well be rather large, since the driving force of second phase formation (from the already growing phases 1 and 3) is often significantly less than that of the first phase formation from one compound and one pure element (see Fig. 4).

5. Nucleation between a growing intermediate phase and a dilute solution

Let L and R be respectively the growing phase 1 and the dilute solution of A in B (β) – Fig. 5. In this case the phase 2 suppression criterion is:

$$\left(\frac{A_1 A_\beta}{A_1 + A_\beta}\right) > \frac{(\Delta g_{20})^2}{10\sigma\Omega}. \quad (28)$$

As before, with

$$A_1 = (C_2-C_1)g_1''\nabla C_1 = w_1\frac{\Delta g_{10}}{\Delta X_1}, \quad (29)$$

and

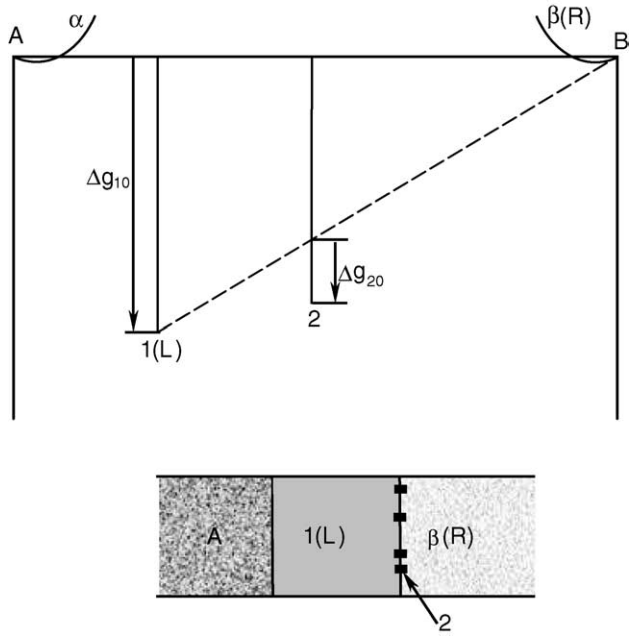

Fig. 5. Schematic representation of phase 2 nucleation between intermediate phase 1 and dilute solution β, already growing in A/B couple. Δg_{10}, Δg_{20} are the driving forces per mole of atoms for the reactions $A + B \rightarrow 1$ and $1 + \beta \rightarrow 2$ respectively.

$$A_\beta = (C_{\beta 1} - C_2) g''_\beta \nabla C_\beta \approx (1 - C_2) \frac{kT}{1 - C_\beta} \nabla C_\beta, \tag{30}$$

$(-\Delta g_{10})$ and $(-\Delta g_{20})$ are the driving forces of reactions $A + B \rightarrow 1$ and $1(L) + B(R) \rightarrow 2$ respectively (see Fig. 5).

To express the gradient in the dilute solution in the presence of growing intermediate phase, it is necessary to solve the following set of algebraic equations for simultaneous parabolic growth of phase 1 layer and of β – solution with parabolic movement of interfaces A/1 and 1/β:

$$C_1 \frac{k_{A1}}{2} = -\frac{D_1 \Delta C_1}{k_{1\beta} - k_{A1}}, \tag{31a}$$

$$(1 - C_1) \frac{k_{1\beta}}{2} = \frac{D_1 \Delta C_1}{k_{1\beta} - k_{A1}} - \sqrt{\frac{D_\beta}{\pi}} (1 - C_{\beta 1}) \frac{\exp(-k_{1\beta}^2 / 4 D_\beta)}{1 - \mathrm{erf}(k_{1\beta} / 2\sqrt{D_\beta})}, \tag{31b}$$

where $y_{A1} = k_{A1}\sqrt{t}$, $y_{1\beta} = k_{1\beta}\sqrt{t}$.

Analytically, two boundary cases can be considered (which are most often encountered):

5.1. $D_\beta \ll D_1 \Delta C_1$ (very low diffusivity in solution, which is usual for high melting B),

5.2. $(1 - C_\beta)^2 D_\beta \gg D_1 \Delta C_1$ (very high diffusivity in solution – low melting B).

Omitting elementary algebra and expansions into Taylor series, the results are given hereafter:

5.1. $D_\beta \ll D_1 \Delta C_1$

In this case:

$$k_{1\beta} \approx \sqrt{\frac{C_1}{1 - C_1}} \sqrt{2 D_1 \Delta C_1},$$

$$\Delta X_1 \approx \sqrt{\frac{1}{C_1 (1 - C_1)}} \sqrt{2 D_1 \Delta C_1 t},$$

$$\nabla C_\beta \approx (1 - C_\beta) \sqrt{\frac{C_1}{1 - C_1}} \sqrt{\frac{2 D_1 \Delta C_1}{(2 D_\beta^2 t)}}, \tag{32}$$

so that

$$A_\beta \approx (1 - C_2) \sqrt{\frac{C_1}{1 - C_1}} \sqrt{2 D_1 \Delta C_1} \frac{k_B T}{2 D_\beta \sqrt{t}},$$

and

$$\frac{A_1}{A_\beta} = \frac{C_2 - C_1}{C_1 (1 - C_2)} \frac{\Delta g_{10}}{k_B T} \frac{D_\beta}{D_1 \Delta C_1} \ll 1. \tag{33}$$

Therefore, $A_1 A_\beta / (A_1 + A_\beta) \approx A_1$ and the suppression criterion is:

$$\frac{\Delta X_1}{l_1^{cr}} < 5 \frac{C_2 - C_1}{C_1 (1 - C_1)} \left(\frac{\Delta g_{10}}{\Delta g_{20}} \right)^2. \tag{34}$$

Thus, in the case of a smaller driving force for the second phase and low diffusivity in B, the thermodynamic suppression of phase 2 may be quite significant.

5.2. $(1 - C_\beta) D_\beta \gg D_1 \Delta C_1$

In this case:

$$k_{1\beta} \cong -\sqrt{\frac{4}{\pi}} (1 - C_\beta) \sqrt{D_\beta} < 0,$$

$$k_{1\beta} - k_{A1} = k = \frac{\Delta X_1}{\sqrt{t}} \approx \sqrt{\frac{\pi}{D_\beta (1 - C_\beta)^2}} \frac{D_1 \Delta C_1}{C_1},$$

$$A_\beta \approx (1 - C_2) \frac{kT}{\sqrt{\pi D_\beta t}},$$

and

$$\frac{A_1}{A_\beta} = \frac{C_2 - C_1}{C_1 (1 - C_2)} \frac{\Delta g_{10}}{k_B T} \frac{D_\beta (1 - C_\beta)}{D_1 \Delta C_1} \gg 1,$$

so that

$$\frac{A_1 A_\beta}{A_1 + A_\beta} \approx A_\beta \approx (1 - C_2) \frac{kT}{\sqrt{\pi D_\beta t}}.$$

This leads to the following suppression criterion:

$$\sqrt{\pi D_\beta t} < 5 (1 - C_2) \frac{k_B T}{\Delta g_{20}} l_2^{cr} < l_2^{cr},$$

so that, in this case, suppression is actually absent.

The best candidates for second phase suppression by chemical potential gradient are therefore the systems

with a considerable difference in melting temperature between constituents. More probably, the first phase to grow will be the phase which is closest to the low-melting-point-element. Then, for the second phase, the situation will be as in Section 5.1.

6. Application

The reactions of metal layers with their silicon substrates resulting in the formation of various silicides are generally considered not only as phenomena common to all diffusion couples where new phases are formed, but also as typical of all transitions from two to three phases [22]. The kinetics of silicide growth are classified into three different categories [22]: diffusion controlled, nucleation controlled and others (reaction rate controlled).

Many silicides such as $Mn_{11}Si_{19}$, $NiSi_2$, $ZrSi_2$, PdSi, $HfSi_2$ etc. have been shown to occur via nucleation-controlled reactions.

The above approach will be applied to (i) Ni–Si, (ii) Co–Si and (iii) Co–Si,Ge thin film systems.

In the following we do not discuss about the nucleation and growth of the first intermediate phase which forms in these systems, i.e., Ni_2Si and Co_2Si [23,24]. These phenomena are discussed in detail elsewhere [2]. Nevertheless, we note that the influence of sharp concentration gradient and/or chemical potentials on nucleation of the first intermediate phase in these systems is insignificant as it is shown in paragraph 3.

We will only discuss the second phase nucleation at the M_2Si/Si interface within the M/M_2Si/Si system (M is here Ni or Si) in (i) and (ii) and the Co_2Si nucleation at the CoSi/Si interface within the Co_2Si/CoSi/Si system in (iii).

(i) In the Ni–Si system, the reaction of nickel with silicon causes the successive formation of Ni_2Si and NiSi at temperatures below 500 °C [23,24]. Ni_2Si grows first at 200 °C and as long as Ni is not completely exhausted, NiSi does not form at the Ni_2Si/Si interface. NiSi grows at about 300 °C only after Ni is exhausted [24].

(Upon the total formation of NiSi – no Ni or Ni_2Si remaining – further heating does not cause any other change until about 800 °C, then one observes the sudden formation of $NiSi_2$; we do not discuss here the $NiSi_2$ nucleation – it has been discussed in detail in [2]).

We discuss here only the NiSi nucleation at the Ni_2Si/Si interface within the Ni/Ni_2Si/Si system (see Fig. 6(b)).

Note that, in this system, the first growing phase is Ni_2Si which is the most stable and simultaneously the compound with highest diffusivity of the three phases (Ni_2Si, NiSi and $NiSi_2$) reported in the thin film systems (see Fig. 6(a)).

For the Ni/Ni_2Si/Si configuration, Eq. (34) can be used to determine the critical thickness of Ni_2Si layer below which nucleation of the NiSi compound at the

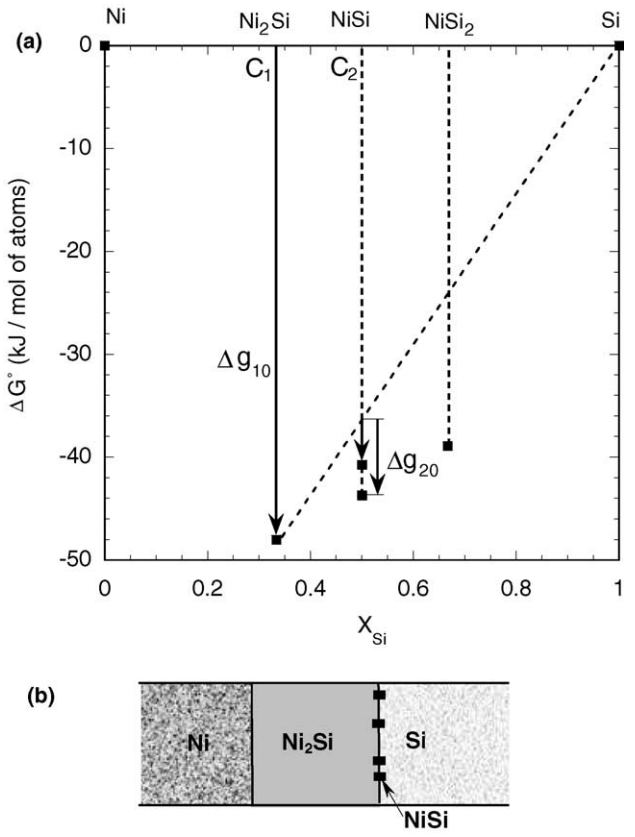

Fig. 6. (a) Gibbs free energy formation of the intermetallic compounds in the Ni–Si system at $T = 600$ K. Δg_{10}, Δg_{20} are the driving forces per mole of atoms for the reactions $2Ni + Si \rightarrow Ni_2Si$ and $Ni_2Si + Si \rightarrow 2NiSi$ respectively. (b) Cross-sectional sketch of the Ni/Ni_2Si/Si system showing localised nucleation of NiSi at the Ni_2Si/Si interface.

Ni_2Si/Si interface is forbidden. The calculations are performed at $T = 600$ K (note that temperature has a very small influence on the values of the Gibbs free energy of phase formation (see Table 1)).

With $C_1 = C_{Ni_2Si} = 1/3$, $C_2 = C_{NiSi} = 1/2$, $\Delta g_{10} = -48$ and $\Delta g_{20} = -4.7$ (−7.7) kJ/mol of atoms [25], the following value is obtained:

$$\frac{\Delta X_{Ni_2Si}}{l^{cr}_{Ni_2Si}} < 5\frac{C_{NiSi} - C_{Ni_2Si}}{C_{NiSi}(C_{Si} - C_{Ni_2Si})}\left(\frac{\Delta g_{10}}{\Delta g_{20}}\right)^2 = \frac{10}{3}\left(\frac{\Delta g_{10}}{\Delta g_{20}}\right)^2 \approx 400(150),$$

$l^{cr}_{Ni_2Si}$ is the critical Ni_2Si nuclei size.

A similar determination can be made in the case of $NiSi_2$ nucleation at the Ni_2Si/Si interface.

This result indicates that, in the Ni/Ni_2Si/Si system, nucleation of NiSi at the Ni_2Si/Si interface is forbidden as long as Ni is not completely consumed and Ni_2Si thickness remains submicronic. In other words:

(a) when the Ni layer is completely consumed, nucleation of NiSi becomes possible regardless of the

Table 1
Experimental values for the standard heat of formation ($\Delta H°$), entropy of formation ($\Delta S°$) and Gibbs free energy formation ($\Delta G°$) of some Ni–Si and Co–Si compounds (from pure elements at 298 K) [24].

Compound	$\Delta H°$ (298 K) (kJ/mol of atoms)	$\Delta S°$ (298 K) (J/mol of atoms)	$\Delta G°$ (600 K) (kJ/mol of atoms)	$\Delta G°$ (1073 K) (kJ/mol of atoms)
Ni_2Si	−48		−48*	
NiSi	−45; −42	−2.1	−43.7; −40,7	
$NiSi_2$	−31	−0.7	−38.9	
Co_2Si	−38		−38*	−38*
CoSi	−48	−3.1	−46.1	−44.7
$CoSi_2$	−33	−1.2	−32.3	−32.6

* Because of the lack of data, $\Delta S° = 0$ is taken.

Ni_2Si thickness (no concentration gradient effect), as observed in thin film experiments [24] and,

(b) when the Ni_2Si thickness becomes greater than a few micrometers, nucleation of NiSi becomes possible even in the presence of Ni layer, as observed experimentally in bulk diffusion reaction experiments [26].

(ii) In the CoSi system, as in the Ni–Si system, Co_2Si grows first at temperatures greater than 200 °C but, in contrast with the Ni–Si system, $CoSi_2$ which forms above 350 °C, grows simultaneously with Co_2Si until all the Co is exhausted. (After the Co layer is completely consumed, the Co_2Si phase dissociates, resulting in the growth of CoSi at the expenses of Co_2Si) [24]. Nevertheless, it maybe noted that, in such case, contrary to the Ni–Si system, the first growing phase is Co_2Si which is not the most stable of the three phases (Co_2Si, CoSi and $CoSi_2$) reported in the thin film systems (see Fig. 7(a)) but has the highest diffusivity.

The coexistence of Co, Co_2Si, CoSi and Si phases and the simultaneous growth of the Co_2Si and CoSi phase are relatively unique features. We discuss here only this simultaneous growth or in other words why the CoSi nucleation is not forbidden at the Co_2Si/Si interface within the Co/Co_2Si/Si system (see Fig. 7(b)). The same determination as in (i), gives the critical thickness of the first growing phase (Co_2Si) beyond which nucleation of CoSi at the Co_2Si/Si interface becomes possible. Calculations are performed here at $T = 600$ K.

With $C_1 = 1/3$, $C_2 = 1/2$, $\Delta g_{10} = -38$ and $\Delta g_{20} = -17.6$ kJ/mol of atoms (see Table 1) [25], the following value is obtained: $\Delta X_{Co_2Si}/l^{cr}_{Co_2Si} < 8$ which means that nucleation of CoSi at the Co_2Si/Si interface becomes possible at a very early stage of Co_2Si growth (ΔX_{Co_2Si} of the order of just a few nanometers), as observed experimentally.

(iii) Film thickness effects in the Co–$Si_{1-x}Ge_x$ solid phase reactions have recently been highlighted by Boyanov et al. [27]: The interfacial products of Co with $Si_{0.79}Ge_{0.21}$ after annealing at 800 °C depend on the thickness of the Co film. Complete conversion to $CoSi_2$ occurred only when the thickness of the Co layer exceeded 35 nm. Interface reactions with Co layers thinner than 5 nm resulted in CoSi formation. The threshold

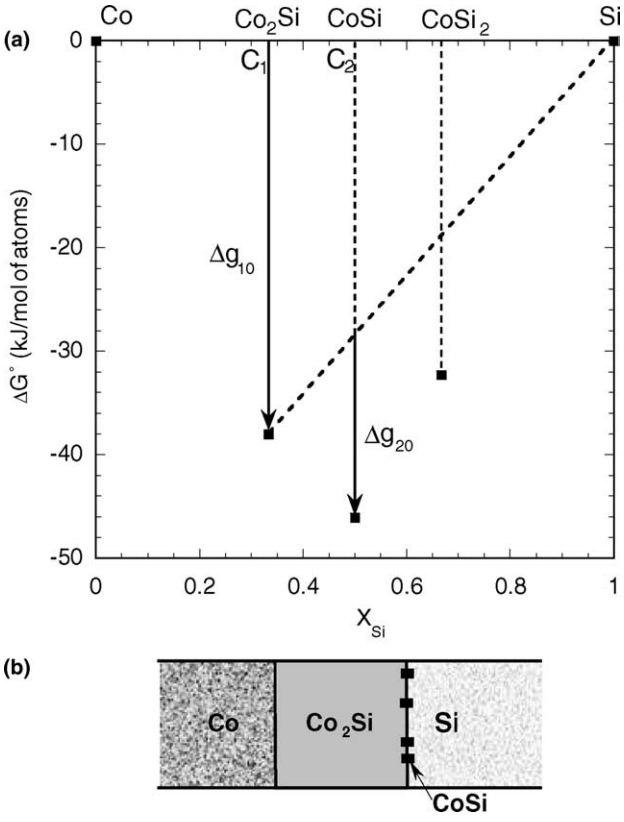

Fig. 7. (a) Gibbs free energy formation of the intermetallic compounds in the Co–Si system at $T = 600$ K. Δg_{10}, Δg_{20} are the driving forces per mole of atoms for the reactions $2Co + Si \rightarrow Co_2Si$ and $Co_2Si + Si \rightarrow 2CoSi$ respectively. (b) Cross-sectional sketch of the Co/Co_2 Si/Si system showing localised nucleation of CoSi at the Co_2 Si/Si interface.

thickness for nucleation of $CoSi_2$ on $Si_{1-x}Ge_x$ was determined in the range $0 \leqslant x \leqslant 0.25$ and increases exponentially with x_{Ge}. The critical initial Co thickness is as high as 22 nm for $x_{Ge} = 0.25$ (Fig. 9(a)).

In order to explain this critical thickness effect, it is assumed in the present approach that, before the $CoSi_2$ nucleation could take place, the system is made up of Co_2Si/CoSi/Si (no Co remaining), as suggested by experimental results obtained by Lau et al. [24] at 300 °C for the Co–Si system.

In such case, nucleation of $CoSi_2$ (phase 2) between the CoSi growing phase (1) and the right-hand phase Si (β) has to be considered. Co_2Si plays the role of the left-hand phase here (see Fig. 8(b)).

We discuss here only the $CoSi_2$ nucleation at the CoSi/Si interface within the Co_2Si/CoSi/Si system at $T = 800$ °C (Fig. 8(b)).

Under these conditions, the suppression criterion of Co_2Si (phase 2) is given by Eq. (34):

$$\frac{\Delta X_{CoSi_2}}{l^{cr}_{CoSi_2}} < 5\frac{C_{CoSi_2} - C_{CoSi}}{C_{CoSi}(C_{Si} - C_{CoSi})}\left(\frac{\Delta g_1}{\Delta g_2}\right)^2 = \frac{10}{3}\left(\frac{\Delta g_1}{\Delta g_2}\right)^2, \tag{35}$$

Δg_1 and Δg_2 are the Gibbs free energy of reactions (36) and (37) respectively:

$$\frac{3}{4}Co_{\frac{2}{3}}Si_{\frac{1}{3}} + \frac{1}{4} \ll Si \gg_{Si,Ge} \rightarrow Co_{\frac{1}{2}}Si_{\frac{1}{2}}, \tag{36}$$

$$\frac{2}{3}Co_{\frac{1}{2}}Si_{\frac{1}{2}} + \frac{1}{3} \ll Si \gg_{Si,Ge} \rightarrow Co_{\frac{1}{3}}Si_{\frac{2}{3}}, \tag{37}$$

with

$$\Delta g_1 = \Delta g_{10} - RT \ln a_{Si}^{1/4} \quad \text{and}$$
$$\Delta g_2 = \Delta g_{20} - RT \ln a_{Si}^{1/3}. \tag{38}$$

The standard Gibbs free energy of reactions (36) and (37) at 800 °C, respectively $\Delta g_{10} = -16.2 \pm 1$ and $\Delta g_{20} = -1.9 \pm 1$ kJ/mol of atoms can be easily calculated from the values of standard Gibbs free energy of formation of Co_2Si, CoSi and $CoSi_2$ phases from pure silicon and cobalt at 800 °C (see Table 1). a_{Si} is the silicon activity in the Si,Ge solid solution which may be considered as an ideal solid solution $a_{Si} \approx C_{Si}$ [28].

Determination, from Eq. (35), of the critical thickness of CoSi layer beyond which the nucleation of $CoSi_2$ between a CoSi layer and Si substrate may take place, shows that this thickness depends strongly on the composition of Si,Ge solid solution, as observed experimentally (see Fig. 9(b)) by Boyanov et al. [27]. Even so, it was noted that these critical thickness values are very sensitive to the standard Gibbs free energy formation of intermediate phases for which experimental errors are of the order of some kJ per mol of atoms.

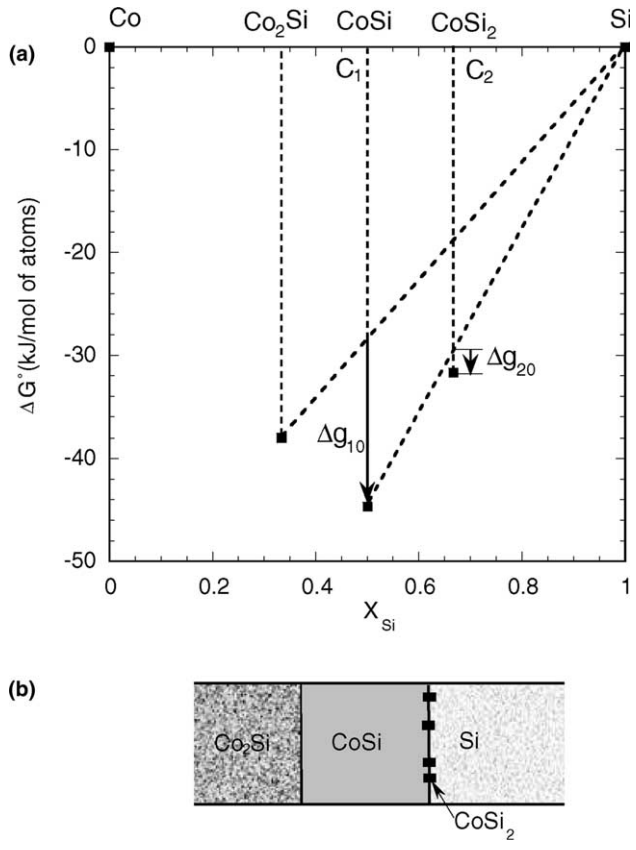

Fig. 8. (a) Gibbs free energy formation of the intermetallic compounds in the Co–Si system at $T = 1073$ K. Δg_{10}, Δg_{20} are the driving forces per mole of atoms for the reactions $Co_2Si + Si \rightarrow 2CoSi$ and $CoSi + Si \rightarrow CoSi_2$ respectively. (b) Cross-sectional sketch of the Co_2Si/CoSi/Si system showing localised nucleation of $CoSi_2$ at the CoSi/Si interface.

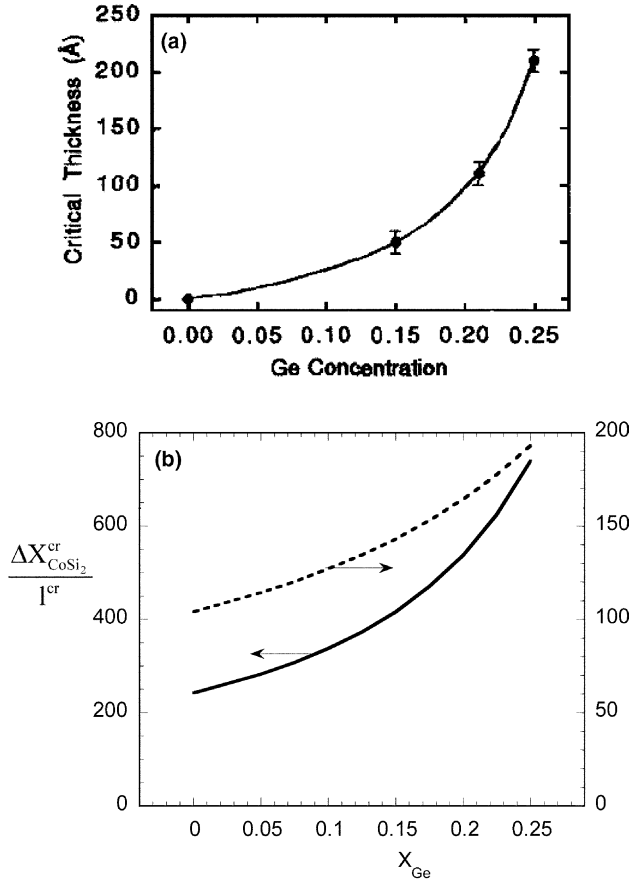

Fig. 9. (a) Experimental values of the critical thickness for $CoSi_2$ nucleation in the $Co/Si_{1-x}Ge_x$ system ($\Delta X^{cr}_{CoSi_2}$) as a function of Ge concentration in Si,Ge solid solution at $T = 800$ °C – from [26]. (b) Calculated values of $\Delta X^{cr}_{CoSi_2}$ from Eqs. (35) and (38) with $\Delta g_{10} = -16.2 \pm 1$; $\Delta g_{20} = -1.9$ (solid line) and $\Delta g_{20} = -2.9$ kJ/mol of atoms (dashed line) – see Fig. 8. l^{cr} is the critical size of $CoSi_2$ nuclei.

7. Conclusion

A new possible explanation for sequential phase growth in thin films is proposed in the context of the "nucleation in concentration gradient" approach. If at least one phase with narrow homogeneity range is already growing, the sharp chemical potential gradient in it strongly influences the nucleation barrier for the next phase to appear. In the expression of Gibbs free energy change, the additional term, due to gradient concentration, appears to be proportional to the fourth power of size instead of the fifth power in previous models (developed for the case of a broad range of parent phase concentration). As a result, thermodynamic suppression of the new phase nucleation (in addition to kinetic suppression) may be effective as long as the thickness of the "suppressing" phase remains less than a few tens or even hundreds of nanometers. Thus, the "gradient term effect" may well lead to the total absence of suppressed phases prior to consumption of the thin film by the "suppressing" growing phase. Comparison with available experimental data demonstrates that the approach presented is at least reasonable.

Acknowledgements

This work is supported by INTAS (grant # 00-784). The authors would like to thank Prof. P. Desré, Prof. P. Gas and Prof. K.N. Tu for helpful discussions. One of the authors (AMG) would like to thank the LTPCM-ENSEEG (Grenoble) for its hospitality. At the last stage of work over this paper one of authors (AMG) was supported by CRDF, grant UE1-2523-CK-03.

References

[1] Tu KN, Mayer JW. Silicide formation. In: Poate JM, Tu KN, Mayer JW, editors. Thin films – inter-diffusion and reactions. John Wiley; 1978 [Chapter 10].
[2] Gas P, d'Heurle FM. Diffusion in silicides: basic approach and practical applications. In: Miglio L, d'Heurle FM, editors. Silicides: fundamentals and applications. Singapore: World Scientific; 2000. p. 34.
[3] van Loo FJJ. Prog Solid State Chem 1990;20:47.
[4] Gusak AM, Gurov KP. Fizika Metallov I Metallovedenie 1982;53:842 [in Russian].
[5] Gusak AM, Lucenko GV. Acta Mater 1998;46:3343.
[6] Gusak AM, Hodaj F, Bogatyrev AO. J Phys Condens Matter 2001;13:2767.
[7] Goesele U, Tu KN. J Appl Phys 1982;53(4):3252.
[8] Gusak AM. Ukrainian Phys J 1990;35(5):725.
[9] Desre PJ, Yavari AR. Phys Rev Lett 1990;64:1533.
[10] Desre PJ. Acta Metall 1991;39:2309.
[11] Gusak AM, Nazarov AV. J Phys: Condensed Matter 1992;4:4753.
[12] Gusak AM, Gurov KP. Solid State Phenomena 1992;23 & 24:117.
[13] Hodaj F, Desre PJ. Acta Mater 1996;44:4485.
[14] Hodaj F, Gusak AM, Desre PJ. Philos Mag A 1998;77:1471.
[15] Hoyt JJ, Brush LN. J Appl Phys 1995;78(3):1589.
[16] Bogatyrev AO. PhD thesis, Institute for Metal Physics, Kiev, 1999.
[17] Gusak AM, Dubiy OV, Kornienko SV. Ukrainian Phys J 1991;36(2):286.
[18] Gusak AM, Lyashenko YuA, Bogatyrev AO. Nucleation at the interphase interface in the process of reactive diffusion. In: Johnson WC, Howe JM, Laughlin DE, Soffa WA, editors. Proceedings of PTM-94, Solid–Solid Phase Transformation. USA: TMS; 1994. p. 1171.
[19] Lee B-J, Hwang NM, Lee HM. Acta Mater 1997;45(5):1867–74.
[20] Bogatyrev AO, Hodaj F, Gusak AM. Bull Cherkasy State Univ – Physics 2001–2002;37 & 38:89.
[21] Raichenko AI. Mathematical theory of diffusion with applications. Kiev. Nauka. Publ.; 1981.
[22] d'Heurle FM. J Mater Res 1998;3(1):167.
[23] d'Heurle FM, Gas P. J Mater Res 1986;1(1):205.
[24] Lau SS, Mayer JW, Tu KN. J Appl Phys 1978;49(7):4005.
[25] de Boer FR, Boom R, Mattens WCM, Miedema AR, Nienssen AK. Cohesion in metals. Transition metal alloys. In: de Boer FR, Pettifor DG, editors. Cohesion and structure. Amsterdam: Elsiever Science Publishers B.V.; 1988.
[26] Gülpen JH, Kodentsov AA, van Loo FJJ. Z Metallkd 1995;86:530.
[27] Boyanov BI, Goeller PT, Sayers DE, Nemanich RJ. J Appl Phys 1998;84(8):4285.
[28] Olesinski RW, Abbaschian GJ. Bull Alloy Phase Diagrams 1984;5(2):180.